

Generation of multicycle terahertz pulses via optical rectification in periodically inverted GaAs structures

Yun-Shik Lee^{a)} and W. C. Hurlbut

Department of Physics, Oregon State University, Corvallis, Oregon 97331-6507

K. L. Vodopyanov and M. M. Fejer

E. L. Ginzton Laboratory, Stanford University, Stanford, California 94305

V. G. Kozlov

Microtech Instruments, Inc., Eugene, Oregon 97403

(Received 3 July 2006; accepted 10 September 2006; published online 30 October 2006)

The authors demonstrate the generation of multicycle narrow-bandwidth terahertz pulses in periodically inverted GaAs structures using optical rectification of 2 μm , 100 fs pump pulses. Three different types of orientation-inverted samples are employed: optically contacted multilayer, orientation-patterned, and diffusion-bonded GaAs. The terahertz pulses are characterized by two-color (pump at 2 μm and probe at 0.8 μm) terahertz time-domain spectroscopy and terahertz Michelson interferometry. © 2006 American Institute of Physics. [DOI: 10.1063/1.2367661]

Many nonlinear materials have been examined for terahertz generation via optical rectification using femtosecond pulses. ZnTe is found to have an excellent property for terahertz generation: the optical group velocity around the 800 nm wavelength range of Ti:sapphire femtosecond lasers matches terahertz group velocities. Consequently, a terahertz pulse generated in ZnTe has a single-cycle wave form with subpicosecond pulse duration—its spectrum is typically broader than 1 THz. On the other hand, narrow-band multicycle terahertz pulses have been generated in the engineered domain structures of periodically poled lithium niobate (PPLN) crystals.¹ Quasiphase matching (QPM) structures such as PPLN consist of a periodic system of domains of alternating crystal orientation. The sign of the second-order nonlinear polarization generated by femtosecond pulses is therefore inverted at the domain boundaries. If the domain length is comparable with the walk-off length $d_w = c\tau / (n_{\text{THz}} - n_{\text{opt}})$ (c : speed of light, τ : optical pulse duration, and n_{opt} and n_{THz} : optical group and terahertz indices of refractions, respectively), QPM between the terahertz wave and the nonlinear polarization extends the interaction length between terahertz and optical pulses.² Both approaches to terahertz generation—phase matching in ZnTe and QPM in PPLN—have similar optical-to-terahertz conversion efficiencies; the power and photon conversion efficiencies are about 10^{-5} and 10^{-3} , respectively.³ In an effort to improve conversion efficiency, the terahertz generation in a new material—periodically structured QPM GaAs—was demonstrated using mid-IR femtosecond pulses.^{4–6}

In this letter, we report the generation of terahertz wave packets in three different types of QPM GaAs, as well as their coherent detection. The mechanism for terahertz generation in our case is the QPM optical rectification, as opposed to the widely used photoconductive antenna technique in GaAs, where terahertz radiation is produced via ultrafast charge transport caused by photoexcitation with femtosecond laser pulses of the near-IR range.^{7–9} GaAs has several advantages for QPM terahertz wave generation, as compared to

PPLN. The foremost is that it is highly transparent at terahertz frequencies (below 1.5 THz the absorption coefficient is less than 1 cm^{-1}).¹⁰ Secondly, the mismatch between the optical group velocity and terahertz phase velocity is much smaller; the corresponding group (n_g) and refractive (n) indices are $n_g = 3.431$ at 2 μm and $n = 3.61$ at 1 THz, respectively. Consequently, the walk-off length is much longer: $d_w = 0.17 \text{ mm}$ for 2 μm , 100 fs pulse. In order to avoid linear and two-photon absorption in GaAs, we use femtosecond pulses at a sufficiently long wavelength of 2 μm . A theoretical calculation indicates that the optimum ratio of a QPM period to a walk-off length for narrow-band terahertz generation is $\Lambda/d_w = 4 \sim 8$.² Outside this range, the terahertz spectrum includes undesirable spectral components such as a broad peak in the lower frequency side or high harmonics, and terahertz field amplitude is less than half of the maximum value at $\Lambda/d_w = 4.2$. The ideal QPM period of GaAs for a 2 μm , 100 fs pulse ranges from 0.7 to 1.4 mm.

We generated terahertz pulses in QPM structures based on optically contacted GaAs (OC-GaAs), diffusion-bonded GaAs (DB-GaAs),¹¹ and all epitaxially grown orientation-patterned GaAs (OP-GaAs).¹² We fabricated the OC-GaAs sample by stacking up four 1-mm-thick, 2-in.-diameter GaAs wafers in a clean room. The DB-GaAs sample, described in Ref. 11, is 6 mm long with a cross section of about $1 \times 1 \text{ cm}^2$ and an average QPM period of 504 μm . The epitaxially grown [molecular beam epitaxy and hydride vapor phase epitaxy (HVPE)] OP-GaAs samples are A10 ($\Lambda = 1277 \mu\text{m}$, $L = 10 \text{ mm}$), A3 ($\Lambda = 1277 \mu\text{m}$, $L = 3 \text{ mm}$), B10 ($\Lambda = 759 \mu\text{m}$, $L = 10 \text{ mm}$), and B6 ($\Lambda = 759 \mu\text{m}$, $L = 10 \text{ mm}$), where Λ is the QPM period and L is the crystal length. The bulk absorption loss of GaAs at 2 THz was measured to be 4.4 cm^{-1} , approximately twice the literature value.¹⁰ The linear absorption was negligible for the $\lambda = 2 \mu\text{m}$ pump, and the samples were non-antireflection-coated. The optical and terahertz beams propagated along the $\langle 110 \rangle$ direction of GaAs.

2 μm pump pulses were produced using an optical parametric amplifier (OPA) system (Coherent Inc., OperA) pumped by a 0.8 μm Ti:sapphire regenerative amplifier (Coherent Inc., Legend). The idler output tuned at 2 μm from the OPA was focused into the QPM crystals with a $1/e^2$

^{a)}Electronic mail: leeys@physics.oregonstate.edu

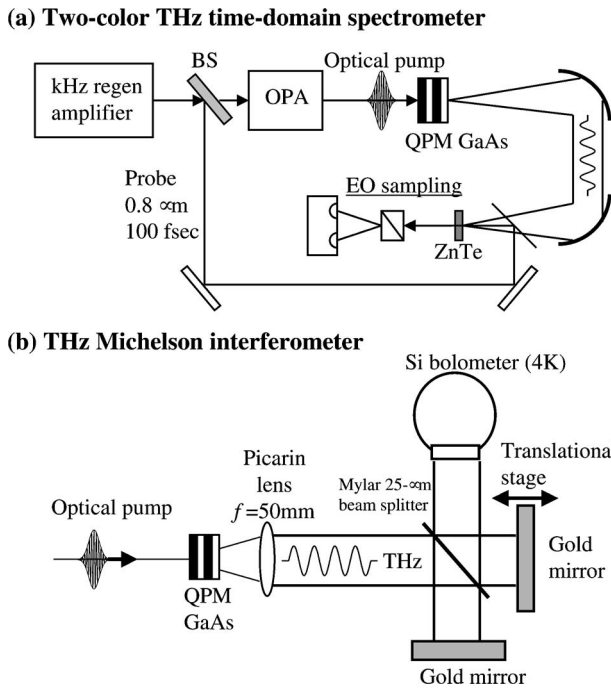


FIG. 1. Experimental setup for (a) two-color terahertz time-domain spectroscopy (pump at 2 μm and probe at 0.8 μm) and (b) terahertz Michelson interferometry.

diameter of $\sim 300 \mu\text{m}$. The typical pulse duration was $\sim 100 \text{ fs}$, repetition rate was 1 kHz, and pulse energy was $> 1 \mu\text{J}$. The optical input power I was kept below $1 \text{ GW}/\text{cm}^2$ at 2 μm in order to avoid three photon absorption (3PA), which can interfere with efficient terahertz generation. For a typical experimental condition of $I = 0.2\text{--}0.5 \text{ GW}/\text{cm}^2$, the absorption loss was less than 5%, which is consistent with the 3PA coefficient of $0.23 \text{ cm}^3/\text{GW}^2$ at 2 μm.¹³ The input power was also far below the measured damage threshold, $\sim 2 \text{ TW}/\text{cm}^2$.

We measured the time-resolved terahertz wave forms using electro-optic sampling in ZnTe with a probe beam from the Ti:sapphire regenerative amplifier. Figure 1(a) shows the two-color terahertz time-domain spectroscopy setup with the pump at 2 μm and the probe at 0.8 μm. The incident optical pulse energy was in the 10 μJ range. We also measured the terahertz absolute power using a Si bolometer (4 K). The terahertz emission from the QPM GaAs samples was collected and collimated by a picarin lens with a 50 mm focal length. The generated terahertz spectral properties were assessed using a Michelson interferometer composed of two gold mirrors and a 25-μm-thick Mylar beam splitter [shown in Fig. 1(b)].

Figure 2 shows the time-resolved terahertz wave forms and corresponding spectra from a 1-mm-thick GaAs wafer and the OC-GaAs structure consisting of four 1-mm-thick GaAs wafers. Single-cycle terahertz pulses were generated in the lone wafer, while 2.5 cycle pulses were produced in the OC-GaAs sample. The spectrum of the terahertz radiation from the OC-GaAs is centered at 0.84 THz (the bandwidth is 0.3 THz), which is consistent with the theoretical calculation, $\nu_{\text{THz}} = c/\Lambda[n(\text{THz}) - n_g(2 \mu\text{m})]$.¹ The terahertz pulse energy from the OC-GaAs sample was measured to be 6.5 times higher than that of the single wafer. For a sample with many QPM periods, the terahertz pulse energy and number of oscillations are proportional to the number of QPM peri-

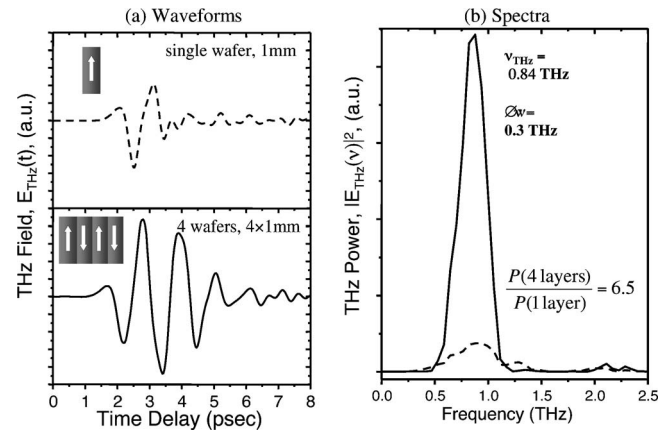


FIG. 2. (a) Time-resolved terahertz wave forms from a 1-mm-thick GaAs wafer and an OC-GaAs sample (a stack of four 1-mm-thick GaAs wafers) and (b) corresponding spectra. Solid and dashed lines indicate the OC-GaAs sample and the single wafer, respectively.

ods because each domain of a QPM structure contributes a half cycle to the terahertz pulse. This simple rule cannot be applied to a sample with a small number of QPM periods because the first and the last domains of a QPM structure contribute more than a half cycle. A numerical simulation shows the effects of the domains near the entrance and exit surfaces.² Due to the contributions from the first and the last layers, the wave form of the two-period sample has 2.5 cycles instead of 2, and the enhancement factor is 6.5 instead of 4.

We tested three OP-GaAs samples with optimum QPM periods for narrow-band terahertz generation. Figure 3 shows time-resolved terahertz wave forms and corresponding spectra of the three OP-GaAs samples: A10 ($\Lambda = 1.277 \text{ mm}$, $L = 10 \text{ mm}$), B6 ($\Lambda = 0.759 \text{ mm}$, $L = 6 \text{ mm}$), and B10 ($\Lambda = 0.759 \text{ mm}$, $L = 10 \text{ mm}$). The terahertz pulse durations for A10, B6, and B10 are 5.0, 3.6, and 6.0 ps, respectively. Due to strong water-vapor absorption lines around 2.2 THz, the terahertz wave forms of B6 and B10 show long tails of free-induction decay. The spectra are centered at 1.5 THz for A10 and 2.1 THz for B6 and B10. By comparing the spectra for B6 and B10, one can see that the spectrum becomes narrower for longer samples, in accord with theory.¹⁴ It should

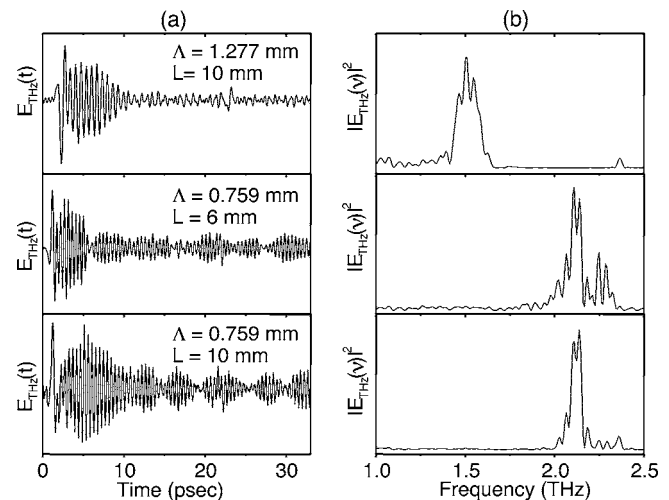


FIG. 3. (a) Time-resolved terahertz wave forms from OP-GaAs samples: A10 ($\Lambda = 1.277 \text{ mm}$, $L = 10 \text{ mm}$), B10 ($\Lambda = 0.759 \text{ mm}$, $L = 10 \text{ mm}$), and B6 ($\Lambda = 0.759 \text{ mm}$, $L = 6 \text{ mm}$) and (b) corresponding spectra.

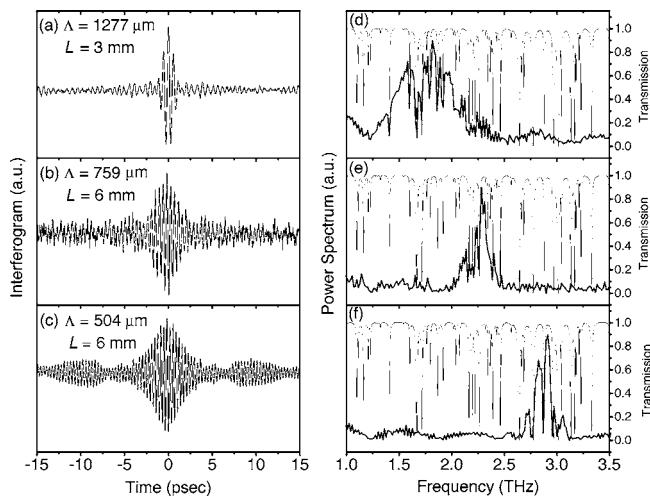


FIG. 4. Michelson interferograms of THz pulses generated by optical excitation at $2.0 \mu\text{m}$ are shown in the left column: (a) A3 ($\Lambda=1277 \mu\text{m}$, $L=3 \text{ mm}$), (b) B6 ($\Lambda=759 \mu\text{m}$, $L=6 \text{ mm}$), and (c) DB-GaAs ($\Lambda=504 \mu\text{m}$, $L=6 \text{ mm}$). Corresponding spectra of the THz pulses extracted from the interferograms are featured in the right column: (d) A3, (e) B6, and (f) DB-GaAs. The spectra are distorted by water-vapor absorption lines (water transmission spectrum is shown on the plots with thin lines).

be mentioned that the spectra of Fig. 3(b) are consistent with Michelson interferometry measurements taken separately.

Figure 4 shows the time-resolved Michelson interferograms of terahertz pulses generated by optical excitation at $2.0 \mu\text{m}$: (a) A3 ($\Lambda=1277 \mu\text{m}$, $L=3 \text{ mm}$), (b) B6 ($\Lambda=759 \mu\text{m}$, $L=6 \text{ mm}$), and (c) DB-GaAs ($\Lambda=504 \mu\text{m}$, $L=6 \text{ mm}$). The corresponding spectra of the terahertz pulses are featured in the right column: (d) A3, (e) B6, and (f) DB-GaAs. The narrow absorption lines in the spectra are consistent with the water transmission spectrum (thin line) superimposed on the plots. The measured (calculated) central frequencies for $\Lambda=1277$, 759 , and $504 \mu\text{m}$ are 1.7 (1.31), 2.2 (2.21), and 2.9 (3.32) THz, respectively. The calculation agrees well with the measurement for B6 and DB-GaAs, but there is a significant discrepancy for A3. There are several reasons for this. First, A3 has only 2.5 QPM periods, so its spectral uncertainty is large. Second, the measured spectrum may be deficient in lower frequency components due to their relatively large diffraction and the finite size of the collecting lens. Agreement between the experiment and the calculation is much better for the emitters with shorter QPM period (higher frequency) and longer sample length (narrower bandwidth).

We have demonstrated the generation of multicycle narrow-bandwidth terahertz radiation based on phase-synchronous optical rectification in periodically inverted GaAs structures such as OC-GaAs, OP-GaAs, and DB-GaAs. We generated terahertz pulses using $2 \mu\text{m}$ femtosecond pump pulses with $\sim 10 \mu\text{J}$ pulse energy and measured the terahertz wave forms via electro-optic sampling in ZnTe

using $0.8 \mu\text{m}$ probe pulses. The corresponding power spectra were also measured by a terahertz Michelson interferometer. Frequency tunability in the range of $0.8\text{--}3$ THz was achieved with several structure periods. Finally, it is worth mentioning the advantages and disadvantages of the three types of the QPM GaAs samples. An OC-GaAs sample is easy to fabricate and has a large clear aperture. However, it is hard to get optically clear interfaces when the number of QPM periods exceed ~ 5 . The diffusion bonding method warrants smooth interfaces and a large clear aperture, but requires highly specialized fabrication techniques. Lastly, the all-epitaxial growth technique gives precise control of the QPM period and clear domain boundaries. Furthermore, it allows complicated domain structures with a submicron resolution. For example, continuous tuning is attainable using OP-GaAs samples with a variable domain-inversion period (fanned out) across the sample.¹⁵ A disadvantage of this technique is a small clear aperture; our sample height was $\sim 1 \text{ mm}$.

The authors would like to thank David Bliss and Candace Lynch (Air Force Research Laboratory, Hanscom, MA) for the thick-film HVPE growth of the OP-GaAs samples. This work was supported by DARPA under Grant No. FA9550-04-1-0465 and by NSF Career Award No. 0449426.

¹Y.-S. Lee, T. Meade, V. Perlin, H. Winful, T. B. Norris, and A. Galvanauskas, *Appl. Phys. Lett.* **76**, 2505 (2000).

²Y.-S. Lee and T. B. Norris, *J. Opt. Soc. Am. B* **19**, 2791 (2002).

³Y.-S. Lee, T. Meade, M. DeCamp, T. B. Norris, and A. Galvanauskas, *Appl. Phys. Lett.* **77**, 1244 (2000).

⁴K. L. Vodopyanov, M. M. Fejer, D. M. Simanovskii, V. G. Kozlov, and Y.-S. Lee, Conference on Lasers and Electro Optics Technical Digest, Baltimore, MD, May 2005 (Optical Society of America, Washington, DC, 2005), Paper No. CWM1.

⁵G. Imeshev, M. E. Fermann, K. L. Vodopyanov, M. M. Fejer, X. Yu, J. S. Harris, D. Bliss, and C. Lynch, *Opt. Express* **14**, 4439 (2006).

⁶K. L. Vodopyanov, M. M. Fejer, X. Yu, J. S. Harris, Y.-S. Lee, W. C. Hurlbut, V. G. Kozlov, D. Bliss, and C. Lynch, *Appl. Phys. Lett.* **89**, 141119 (2006).

⁷X.-C. Zhang, B. B. Hu, J. T. Darrow, and D. H. Auston, *Appl. Phys. Lett.* **56**, 1011 (1990).

⁸B. B. Hu, X.-C. Zhang, and D. H. Auston, *Phys. Rev. Lett.* **67**, 2709 (1991).

⁹M. B. Johnston, D. M. Whittaker, A. Corchia, A. G. Davies, and E. H. Linfield, *Phys. Rev. B* **65**, 165301 (2002).

¹⁰D. Grischkowsky, S. Keiding, M. van Exter, and Ch. Fittinger, *J. Opt. Soc. Am. B* **7**, 2006 (1990).

¹¹L. A. Gordon, G. L. Woods, R. C. Eckardt, R. R. Route, R. S. Feigelson, M. M. Fejer, and R. L. Byer, *Electron. Lett.* **29**, 1942 (1993).

¹²L. A. Eyres, P. J. Tourreau, T. J. Pinguet, C. B. Ebert, J. S. Harris, M. M. Fejer, L. Becouarn, B. Gerard, and E. Lallier, *Appl. Phys. Lett.* **79**, 904 (2001).

¹³W. C. Hurlbut, K. L. Vodopyanov, P. S. Kuo, M. M. Fejer, and Yun-Shik Lee, Conference on Lasers and Electro Optics Technical Digest, Long Beach, CA, May 2006 (Optical Society of America, Washington, DC, 2006), Paper No. QThM3.

¹⁴K. L. Vodopyanov, *Opt. Express* **14**, 2263 (2006).

¹⁵W. C. Hurlbut, B. J. Norton, N. Amer, and Yun-Shik Lee, *J. Opt. Soc. Am. B* **23**, 90 (2006).